ACS APPLIED MATERIALS & INTERFACES



Article

# Probing the dynamic interaction between damaged DNA and a cellular responsive protein using a piezoelectric mass biosensor

Yulong Jin, Yunfeng Xie, Kui Wu, Yanyan Huang, Fuyi Wang, and Rui Zhao

*ACS Appl. Mater. Interfaces*, **Just Accepted Manuscript** • DOI: 10.1021/acsami.6b15077 • Publication Date (Web): 20 Feb 2017



ACS Publications

ACS Applied Materials & Interfaces is published by the American Chemical Society.
1155 Sixteenth Street N.W., Washington, DC 20036

# Probing the dynamic interaction between damaged DNA and a cellular responsive protein using a piezoelectric mass biosensor

*Yulong Jin,[†‡] Yunfeng Xie, [†‡#] Kui Wu,[†‡] Yanyan Huang,*[†‡] Fuyi Wang,*[†‡] and Rui Zhao*[†‡]*

[†] *Beijing National Laboratory for Molecular Sciences, CAS Key Laboratory of Analytical Chemistry for Living Biosystems, Institute of Chemistry, Chinese Academy of Sciences, Beijing, 100190, China.*

[‡] *University of Chinese Academy of Sciences, Beijing 100049, China.*

KEYWORDS: DNA damage, piezoelectric mass biosensor, high mobility group box 1, molecular recognition, kinetic analysis

ABSTRACT: The binding events between damaged DNA and recognition biomolecules are of great interest for understanding of the activity of DNA-damaging drugs and the related DNA repair networks. Herein, a simple and sensitive sensor system was tailored for real-time probing the dynamic molecular recognition between cisplatin-damaged DNA (cisPt-DNA) and a cellular responsive protein, high mobility group box 1 (HMGB1). By integrating of flow injection analysis (FIA) with quartz crystal microbalance (QCM), the interaction time-course of cisPt-DNA and HMGB1 domain A (HMGB1a) was investigated. The highly specific sensing interface

was carefully designed and fabricated using cisPt-DNA as recognition element. A hybrid self-assembled monolayer consisting cysteamine and mercaptohexanol was introduced to resist non-specific adsorption. The calculated kinetic parameters ($k_{ass}$ and $k_{diss}$) and the dissociation constant ($K_D$) demonstrated the rapid recognition and tight binding of HMGB1a towards cisPt-DNA. Molecular docking was employed to simulate the complex formed by cisPt-DNA and HMGB1a. The tight binding of such DNA-damage responsive complex is appealing for the downstream molecular recognition event related with the resistance to DNA repair. This continuously-flow QCM biosensor is an ideal tool for studying specific interactions between drug-damaged DNAs and their recognition proteins in physiological-relevant environment, and will provide a potential sensor platform for rapid screening and evaluating metal anticancer drugs.

## INTRODUCTION

DNA damage, as a trigger for cell death, is one of the main strategies in cancer chemotherapy.[1,2] Many clinically used anticancer drugs including platinum-based drugs, doxorubicin and mitomycin take effect on DNA. As the response to DNA damage, cells have developed delicate and complicated molecular interaction network to modulate the downstream pathways, such as DNA damage repair, damage tolerance or apoptosis.[3-6] Among these, molecular recognition events that block DNA repair processes thus determine the effectiveness of therapy emerge as a highlighted research field.

To understand the initial signals in DNA damaging response, the binding events between the DNA-drug complex and the recognition biomolecules are extensively investigated by using affinity ligands.[7-9] The photoaffinity labeling technique enabled the discovery of high-mobility group protein B (HMGB) for the recognition of cisplatin-damaged DNA.[7] Recently, based on affinity gold nanoparticles and mass spectroscopy approach, nuclear protein positive cofactor

PC4 was characterized as the protein responding to *trans*-platinum cross-linked DNA.[10] Despite the great advances in revealing the cellular response proteins to DNA damage, the details of molecular interactions especially in terms of the dynamic recognition processes still lack of investigation.[11] To investigate the kinetic interaction of DNA-HMGB1 complex, stop-flow analysis has been reported to access the biomolecular interactions.[12,13] However, complicated fluorescence labeling is required, which makes the process labor-intensive and may affect the activity of biomolecules. Therefore, label-free, sensitive and real-time analysis of molecular recognition process in physiological relevant conditions is of great importance but continues to be a challenge.

Quartz crystal microbalance (QCM) capable of sensing the mass loading on the crystal surface at the nanogram level has attracted wide attention in the fields of material science,[14,15] biophysics,[16-19] organic reactions[20] and bioanalysis.[21-25] Combining with flow injection analysis technique (FIA), QCM becomes a powerful platform for on-line detection of recognition process of biological molecules in a label-free fashion.[26-28] The FIA-QCM sensing system has demonstrated its effectiveness to analyze the kinetic processes of biomolecular binding events with the attempt to understand the structural/functional relationships.[29,30]

The high-mobility-group box 1 (HMGB1) was a chromatin architectural factor having two tandem DNA-binding domains designated A and B.[31] It has been confirmed that both of the domains can specifically bind to 1,2-intrastrand cross-linked DNA by cisplatin with domain A having a little higher affinity than domain B to the cisplatin-DNA adduct.[3,31,32] The binding of HMG (high mobility group)-domain proteins to cisplatin-damaged DNA has been postulated to mediate the antitumor properties of the drugs. However, the binding kinetics between cisplatin damaged DNA and HMGB1 has not yet been well studied and remains unclear.

In current work, we presented a sensitive and effective method for real-time studying the specific molecular recognition and interaction between damaged DNA and cellular responsive proteins using the FIA-QCM biosensing system. To understand the mechanism of the cisplatin cross-linked DNA (cisPt-DNA) and its recognizable protein HMGB1 at molecular level, a highly selective sensing interface was fabricated with cisPt-DNA complex as biological recognition element. The dynamic association rate constant ($k_{ass}$), dynamic disassociation rate constant ($k_{diss}$) and equilibration dissociation constant ($K_D$) of cisPt-DNA binding to the domain A of HMGB1 (HMGB1a) were calculated through kinetic analysis. With the attempt to understand the structural elements underlying such kinetic behavior, further investigation into the binding conformations of the cisPt-DNA and HMGB1a complex was carried out by molecular modeling.

## EXPERIMENTAL SECTION

### Materials and Apparatus

Cysteamine hydrochloride, 6-Mercapto-1-hexanol (MCH), bovine serum albumin (BSA), human serum albumin (HSA), lysozyme (LZM), human immunoglobulin (hIgG) were all purchased from Sigma (USA). HMGB1a (molecular weight is 9812.3 Da and the isoelectric point (pI) is 10.1) was expressed and purified as a gift from professor Yangzhong Liu at University of Science and Technology of China.[33] Cisplatin was obtained from Alfa Aesar (USA). The single-stranded DNA fragment (5′-CCTCTCTGGACCTTCC-3′, ssDNA **I**), of which the two adjacent GG bases can bind to cisplatin to form a 1,2-intrastrand cross-linked DNA adduct, and its complementary strand with 5′-terminal thiol-modification (5′-SH-$(CH_2)_6$-GGAAGGTCCAGAGAGG-3′, ssDNA **II**) were purchased from TaKaRa (Dalian, China). HMGB1a and the single stranded DNA were dissolved in 50 mmol $L^{-1}$ triethylammonium acetate (TEAA) buffer and kept in -20°C freezer. All other chemicals were of analytical grade

and used without further disposal. Unless otherwise mentioned, all solutions were prepared in TEAA buffer. Water was obtained from a Milli-Q gradient system (Millipore Inc., USA).

The home-made FIA-QCM system used in this study was previously described in detail.[27,34] Briefly, the FIA-QCM system consisted of a flow-through cell (50 μL internal volume), a frequency oscillator (powered by 3V dc), a frequency counter (Model EE3386 universal counter, Nanjing Telecommunication Instrument Factory, Nanjing, China), an infusion pump (Model KDS 100, KD Scientific Inc., Holliston, USA), a HPLC injection valve (Rheodyne 7125, California, USA) and a computer with an in-house kinetic analysis software to record the frequency continuously. The AT-cut quartz crystals (12.0 mm diameter, 10 MHz resonant frequency) with gold electrodes (6.0 mm diameter) on both sides were purchased from Beijing Chenjing Radio Electronic Co., Ltd. (Beijing, China).

**Preparation of QCM biosensor**

The gold surfaces were first treated with Piranha solution ($H_2SO_4$:30% $H_2O_2$=3:1, v/v), rinsed with water and dried in nitrogen stream. Two ways were carried out to immobilize double stranded DNA (dsDNA) onto QCM crystal. In the first way, 50 μL of thiol-labeled ssDNA **II** (1 nmol $L^{-1}$) were dropped onto the cleaned gold crystals overnight at 4 $^{o}$C to form a self-assembled monolayer of the ssDNA. Next, 50 μL of ssDNA **I** (5 nmol $L^{-1}$) were dropped onto gold surface containing ssDNA **II** monolayer. Then the crystals were heated in water bath for 10 min at 70 °C, slowly cool down to room temperature to hybrid dsDNA after removing heat source. Finally, 50 μL of cisplatin solution (100 nmol $L^{-1}$) were dropped onto the dsDNA immobilized crystals surface, and kept for 24 h at room temperature to form cisplatin-DNA adduct. In the second way, cisplatin cross-linked ssDNA **I** (cisPt-**I**) was first prepared and purified as described in the literature.[35] Next, the platinated strand **I** and the thiol-labeled strand **II** were mixed with molar

ratio of 1:1.5. The mixture was heated in water bath for 10 min at 70 °C, then slowly cooled down to room temperature to form cisplatin cross-linked double stranded DNA (cisPt-DNA) complex after removing heating source. Finally, 50 μL of prepared thiol-labeled cisPt-DNA complex were dropped onto the freshly cleaned gold surface, and self-assembled for 12 h at 4 °C. A control sensor was also parallelly fabricated by fixing the undamaged dsDNA onto the sensor surface.

In order to eliminate the non-specific adsorption of proteins onto the sensor, different surface blocking methods were investigated, including BSA blocking and cysteamine/MCH blocking. The blockings were carried out after the cisPt-DNA immobilization. For BSA blocking, a solution containing 0.25 mg/mL BSA was dropped onto gold surface and incubated for 2 h at 37 $^{o}$C. For cysteamine/MCH blocking, the dsDNA-modified gold crystal were immersed into a mixture solution containing 20 mmol $L^{-1}$ cysteamine and 1 mmol $L^{-1}$ MCH, then incubated for 2 h at room temperature in dark. After blocking, the crystal surface was rinsed with large amount of TEAA buffer to get rid of residual solution after the reaction. Blank sensors were also made only by modifying BSA and cysteamine/MCH on the bare crystals, respectively.

**FIA-QCM detection procedures**

The cisPt-DNA immobilized QCM crystal was mounted in the flow through system by two silicon rubber O-rings and rinsed with carrier buffer (50 mmol $L^{-1}$ TEAA-100 mmol $L^{-1}$ $NaClO_4$) continuously at a flow rate of 30 μL $min^{-1}$. After a stable baseline was achieved, 300 μL of HMGB1a solution in a series of dilutions were injected into the fluid system via the injection valve. The curves of frequency versus time were recorded and the binding process of HMGB1a and cisPt-DNA was monitored in real time. After each measurement, the QCM biosensor surface

was regenerated for next determination by injecting 600 μL $NaClO_4$ solution (2 mol $L^{-1}$) to dissociate the bound HMGB1a.

**Molecular docking**

Protein-DNA docking studies were carried out using Hex 8.0.0 program. Structures were modeled using 3D parametric functions which encoded surface shape, electrostatic charge and potential distribution. During the docking, both HMGB1a protein and DNA strands were permitted to move and rotate along x, y and z directions. With the fast Fourier transform (FFT) based docking approach, binding modes with the most favorable binding energies were evaluated. The crystal structures of HMGB1a and cisPt-DNA complex were extracted from the protein data bank (PDB 1CKT). All water molecules were deleted, and polar hydrogen atoms were added to HMGB1a. Finally, the docking results were re-constructed by Pymol.

## RESULTS AND DISCUSSION

**Design and fabrication of sensing interface**

The preparation procedure of the QCM sensor is illustrated in Scheme 1. Thiol-functionalized DNA was used to modify the gold surface of QCM crystal. Two different strategies were designed to establish the cisplatin damaged DNA recognition layer on the sensor surface. For the first approach, as shown in Scheme 1a, the thiol-labeled ssDNA **II** was firstly self-assembled onto the crystal surface to form the monolayer of ssDNA, then the complementary-ssDNA **I** was added for *in situ* hybridization. After annealing, cisplatin was dropped onto sensor surface to induce the 1,2-intrastrand d(GpG) cross-links. Thus the cisPt-DNA functionalized QCM biosensor was obtained. According to the frequency shifts, the signal decrease caused by ssDNA **II** self-assembly and DNA hybridization were 39 ± 3 Hz and 19 ± 8 Hz, respectively (n = 5). The density of ssDNA **II** and **I** on gold surface was calculated as (2.0 ± 0.15) × $10^{13}$ molecules $cm^{-2}$

and $(1.1 \pm 0.45) \times 10^{13}$ molecules $cm^{-2}$, respectively, based on Sauerbray equation.[36] Since the increased mass on the crystal surface totally resulted from the complementary DNA strand involved hybridization reaction, DNA hybridization efficiencies can be calculated to be as 55%.

The second functionalization approach is illustrated in Scheme 1b. In a tube, the cisplatin-cross-linked ssDNA **I** (cisPt-**I**) was firstly prepared, followed by the hybridization of cisPt-**I** with the thiol-modified ssDNA **II** in solution. After the formation of cisPt-DNA complex, cisPt-DNA containing thiol at 5′-terminal was assembled onto the gold surface. QCM frequency decrease caused by cisPt-DNA complex was 30 ± 3 Hz (n = 5) and the corresponding surface density was $(8.1 \pm 0.8) \times 10^{12}$ molecules $cm^{-2}$, which is lower than that of the first approach. Concerning the overall immobilization efficiency, although the first approach yields higher immobilization density, the effect from steric hindrance would hamper the molecular interaction between damaged-DNA and protein. The residual 45% ssDNA in the first approach may interfere the interaction between cisPt-DNA and HMGB1a (Scheme 1a). More importantly, the cross-links formed by cisplatin drugs could occurred in both dsDNA and ssDNA strands in the first approach since both of the ssDNA **I** and **II** have adjacent guanine base (1,2-GG) motifs, which may affect accurate interaction data between HMGB1a and cisPt-DNA. In comparison, in the second approach, the ssDNA **I** 5′-CCTCTCTGGACCTTCC-3′ only contains two G bases ($G_8$ and $G_9$). After incubation with cisplatin, cisplatin induced cross-link is controllable and only happened intrastrand to $G_8$-$G_9$ base in ssDNA **I**. Based on the above considerations, the second immobilization method is ideal and chosen in further study.

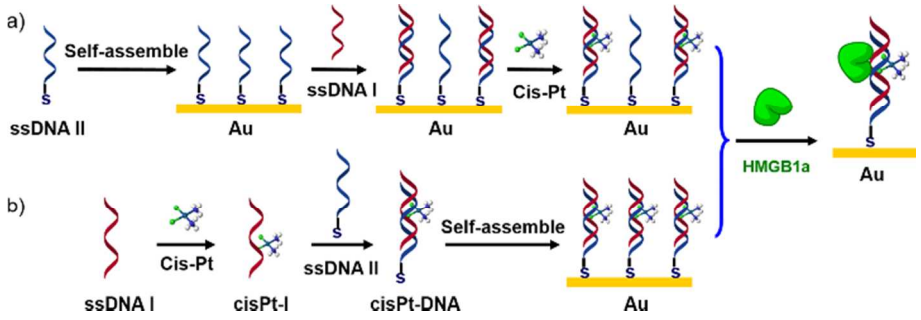


**Scheme 1.** Schematic illustration of two approaches for the immobilization of cisPt-DNA on the sensor interface. (a) ssDNA **II** was self-assembled firstly on sensor surface and hybridized with ssDNA **I** and then the formed dsDNA was cross-linked with cisPt. (b) CisPt cross-linked ssDNA **I** was firstly hybridized with ssDNA **II** and then the cisPt-DNA complex was self-assembled on sensor surface.

**Resisting the non-specific adsorption of HMGB1a**

Before applying the sensor for DNA-damage responsive protein sensing, the non-specific adsorption of the protein on the bare gold surface was examined (Figure 1a). A frequency decrease of 42 Hz was caused by HMGB1a injection. To eliminate such non-specific adsorption, traditional BSA blocking was firstly used to resist non-specific binding. After BSA treatment, the signal change induced by HMGB1a was reduced to only 3 Hz on the blank crystal (Figure 1b). However, such BSA treatment also blocked the interaction between cisPt-DNA and HMGB1a. The frequency change from cisPt-DNA immobilized sensor upon HMGB1a injection was 7 Hz, indicating little binding of HMGB1 to cisPt-DNA (Figure 1b). This phenomenon may be most probably attributed to the steric hindrance from BSA blocker molecules. The three-dimensional of BSA molecule is 5.5 × 5.5 × 9 nm,[37] while the theoretical chain length of dsDNA containing 16 bases pairs is around 5 nm. Therefore, the large size of BSA leads to the shielding of cisPt-DNA and thus failure in HMGB1a binding.

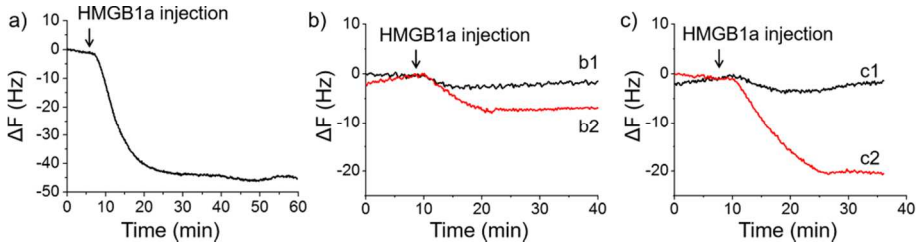


**Figure 1.** Fabrication of sensing interfaces with minimal non-specific adsorption. (a) Adsorption of HMGB1a on bare QCM surface. (b) Binding behavior of HMGB1a on BSA blocked (b1) blank crystal and (b2) cisPt-DNA immobilized sensor. (c) Binding behavior of HMGB1a on cysteamine/MCH blocked (c1) blank crystal and (c2) cisPt-DNA immobilized sensor. [HMGB1a] = 1 μM.

The non-specific adsorption of proteins on sensor surface is closely related with the physiochemical property of the surface. Increasing the amount of hydrophilic groups on gold surface can efficiently resist non-specific adsorption of proteins.[38] Moreover, regulating the charge of functional groups to make it electrically neutral or carrying same charge as binding proteins can also reduce non-specific adsorption.[39,40] With this regard, cysteamine with small size and hydrophilic terminal group can be an ideal candidate. Its thiol group can easily self-assembled onto gold surface of QCM crystal, while the amine group carries positive charge for resisting the adsorption of positively charged HMGB1a (pI = 10.1). The small size of cysteamine will not block the recognition sites on cisPt-DNA. In order to prevent flattening of the immobilized DNA chains on gold surface, 6-mercapto-1-hexanol (MCH) was also added as the blocking reagent. The molar ratio of cysteamine and MCH was optimized as 20:1. After treated with this blocking cocktail, a significant frequency shift of 21 Hz was detected after the injection of HMGB1a to cisPt-DNA modified sensor, while frequency decrement was only 4 Hz on the corresponding blank sensor (Figure 1c). The results thereby proved that cysteamine/MCH hybrid

self-assembled monolayer can not only effectively resist non-specific adsorption, but also has negligible interference with recognition sites on cisPt-DNA complex to HMGB1a.

**Specificity and sensitivity of the sensor**

To evaluate the specificity of the QCM biosensor, proteins with different molecular weights and isoelectric points including HMGB1a, BSA, HSA, hIgG and LZM were injected successively into the FIA-QCM sensing system (5 μM, each). As shown in Figure 2a, the frequency shifts upon the injection of the control proteins are all lower than 10 Hz, which finally returned to the baseline with the rinsing of carrier buffer. On the contrary, the frequency decrease caused by HMGB1a was around 36 Hz. Even rinsed with carrier buffer for 20 min, the frequency kept constant. These results indicated no interaction between cisPt-DNA and BSA, HSA, hIgG, LZM proteins, and manifested the high selectivity of the FIA-QCM sensor towards HMGB1a.

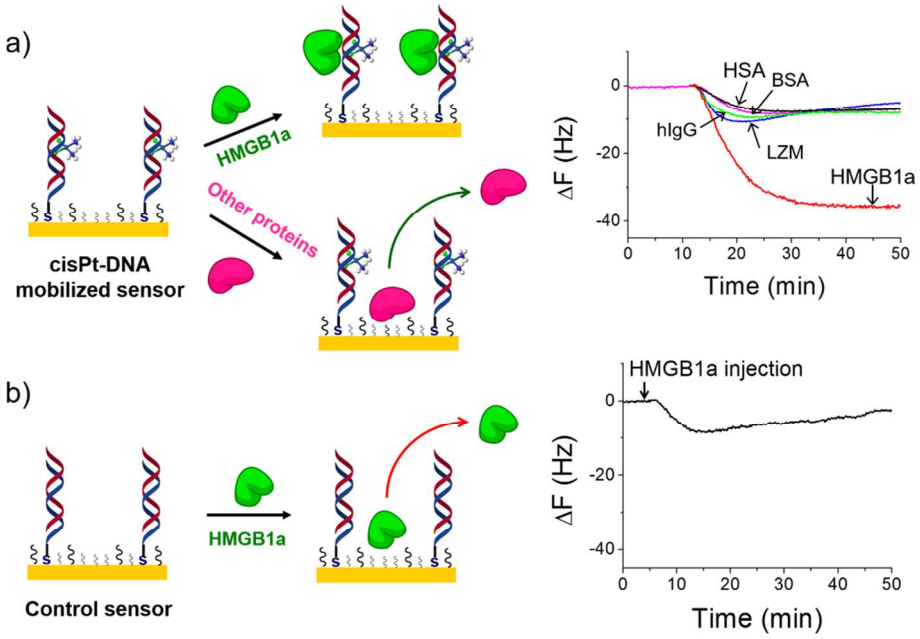


**Figure 2.** The selectivity of the sensor for detecting the binding between cisPt-DNA and HMGB1a. (a) Illustration and sensing of the binding behavior of BSA, HSA, hIgG, LZM and HMGB1a towards cisplatin damaged DNA on sensor. (b) Illustration and sensing of the binding

behavior of HMGB1a towards non-damaged dsDNA immobilized sensor. The concentration of each protein is 5 μM.

To specify that the sensing signal is caused by the recognition of HMGB1a towards cisplatin damaged-DNA, control sensor prepared with non-damaged dsDNA was also examined. As displayed in Figure 2b, although slight frequency change was detected upon HMGB1a injection at the beginning, the sensing curve gradually resumed to baseline, and the final frequency decrease was only 3 Hz. Such negligible response indicated that HMGB1a cannot bind to dsDNA without cisplatin binding. These results clearly confirmed that HMGB1a protein specifically recognize the cisplatin-damaged DNA with an intrastrand cross-link.

The sensitivity of the biosensor was further investigated by monitoring the frequency response caused by the binding of HMGB1a at various concentrations on the QCM biosensor. With increasing concentration of HMGB1a, the trends of frequency response exhibited typical saturated binding curve (Figure 3a). When the HMGB1a concentration was 4 μM, the signal change almost reached saturation. A linear range (R = 0.979) of 0.2-2 μM was obtained (insert of Figure 3a). The limit of detection for HMGB1a is estimated to be down to 60 nM (S/N = 3), indicating the high sensitivity of the sensor for the detection of HMGB1a and its feasibility for studying the binding kinetics between HMGB1a and cisPt-DNA complex.

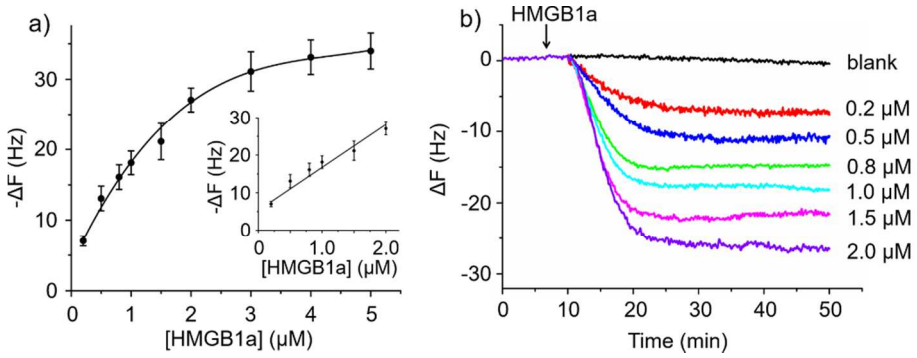

**Figure 3.** (a) Frequency changes of the cisPt-DNA immobilized sensor responding to different concentration of HMGB1a. Insert: diagram of the linear relationship between frequency change and the concentration of HMGB1a. Data were from three parallel experiments. The signal of noise is 0.2 Hz, which was calculated based on the standard deviation of eleven base line shifts of blank sample in 1 h.[41] (b) Typical time-dependent sensing curves of the cisPt-DNA immobilized sensor responding to various concentration of HMGB1a ranging from 0-2.0 μM.

**Binding Kinetics of HMGB1a to damaged DNA**

The kinetics of the interaction between HMGB1a and cisplatin damaged DNA was monitored in real-time, based on the ability of QCM in detecting subtle mass changes associated with biological processes at the interface. The reaction between ligand immobilized on crystal surface and analyte in solution is often assumed to follow pseudo-first-order kinetics, which can be described as the following generalized equation (1):[20,42]

$$\frac{d\theta}{dt} = k_{ass}(1-\theta)C - k_{diss}\theta \quad (1)$$

Under equilibrium conditions, the equation (1) can be reformed to equation (2),

$$\theta = \frac{k_{ass}C}{k_{ass}C + k_{diss}} \quad (2)$$

From the kinetic point of view, integration of equation (1) yields the time fraction of surface coverage as a function of time:

$$\theta(t) = \frac{C}{C + (k_{diss}/k_{ass})}[1 - \exp(-(k_{ass}C + k_{diss})t)] \quad (3)$$

By substituting $k_{obs}=k_{ass}C+k_{diss}$ and $\theta(\infty) = C/[C + (k_{diss}/k_{ass})]$, equation (3) can be simplified to:

$$\theta(t) = \theta(\infty)[1 - \exp(-k_{obs}t)] \quad (4)$$

Assuming that there is a linear relation between $\theta(t)$ and $\Delta F$, according to Sauerbrey equation, equation (4) can be rewritten in terms of the measured frequency difference ($\Delta F$) as follows:

$$\Delta F_t = \Delta F_e[1 - \exp(-k_{obs}t)] \quad (5)$$

For association constant ($K_A$) and dissociation constant ($K_D$),

$$K_A = k_{ass}/k_{diss} \qquad K_D = k_{diss}/k_{ass} \quad (6)$$

Where $\theta$ is the fraction of surface covered, $(1 - \theta)$ is the fraction of surface exposed, $C$ is the concentration of analyte in solution, $k_{ass}$ and $k_{diss}$ are the association rate constant and disassociation rate constant, respectively. $\Delta F_t$ is the frequency shift at time $t$ and $\Delta F_e$ is the frequency shift at time $t \rightarrow \infty$, $K_A$ is association constant and $K_D$ is dissociation constant.

The binding processes of HMGB1a towards cisplatin damaged DNA were monitored in various concentrations (0.2, 0.5, 0.8, 1.0, 1.5 and 2.0 μM) (Figure 3b). The observed rate constants $k_{obs}$ in different concentrations of HMGB1a can be extracted by fitting the experimental binding curves with equation (5) using nonlinear regression analysis.[34] As an example, Figure 4a shows a representative fitting curve of the binding between 0.5 μM HMGB1a and cisPt-DNA complex. By linear fitting $k_{obs}$ versus C (Figure 4b), the kinetic constants of $k_{ass}$ and $k_{diss}$ were easily obtained as $(2.97 \pm 0.21) \times 10^3$ L mol$^{-1}$ s$^{-1}$ and $(8.47 \pm 1.91) \times 10^{-4}$ s$^{-1}$, respectively. These results implied that the interaction between HMGB1a and cisPt-DNA was a fast association and slow dissociation process. The association constant ($K_A$) was calculated as $(3.50 \pm 0.84) \times 10^6$ L mol$^{-1}$, i.e. the dissociation constant ($K_D$) was $(2.86 \pm 0.67) \times 10^{-7}$ mol L$^{-1}$. The fast association and the slow dissociation process suggested the rapid recognition and tight binding of HMGB1a to the cisplatin damaged DNA. Such specific and strong binding event

made HMGB1a shield the cisplatin damaged DNA from intracellular repair and guaranteed the cytotoxic effect of cisplatin towards cancer cells.[31,43]

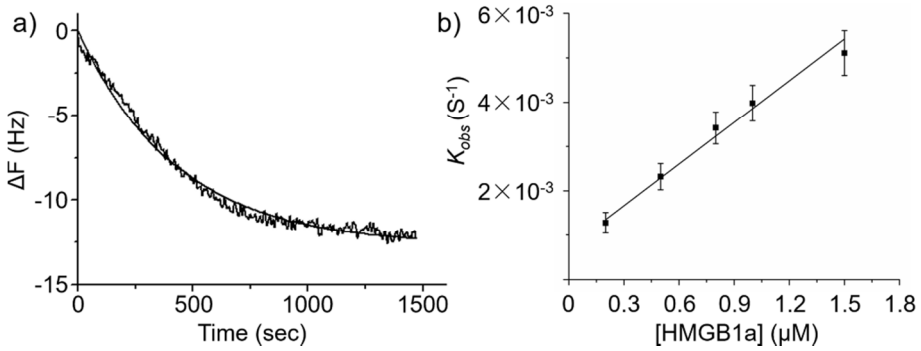


**Figure 4.** (a) A representative binding curve (dotted line) and fitting curve (solid line) for binding HMGB1a (0.5 μM) to cisPt-DNA immobilized QCM crystal. (b) Linear correlation of rate constant $k_{obs}$ against the concentration of HMGB1a.

Due to the biological significance of DNA-HMGB1 interactions, many classic methods have been used,[13,32,44] which provide comprehensive thermodynamic information on protein-DNA complexes. The values of calculated equilibrium dissociation constant ($K_D$) were in the range of nanomolar to micromolar level depending on the different DNA sequences and sensitivity of the methods. In this work, the combination of FIA with QCM provides a continuous-flow system for the real-time analysis of the binding between cisplatin damaged DNA and HMGB1. Both kinetic and thermodynamic information of the interactions between cisplatin crosslinked DNA and HMGB1 were obtained simultaneously in biological-like environments. The obtained $K_D$ value is in good agreement with that from the stopped-flow fluorescent method ($K_D$ = 2.77 ± 1.31) × $10^{-7}$ mol $L^{-1}$),[12] demonstrating the effectiveness of our FIA-QCM method.

**Molecular docking**

The specific interaction between HMGB1a and cisPt-DNA were further simulated by computer modeling software, Hex 8.0 program. Based on 3D fast Fourier transforms (FFTs) algorithm, the program gave the interaction energy (E-value) between HMGB1a and cisPt-DNA by considering shape density, electrostatic charge scoring, and potential scoring.[45] The most favorable binding mode should give the lowest E-value and indicated the formation of the most stable complex. Given typical DNA sequence and cisplatin cross-linking procedure in this study (Scheme 1b), cisplatin induced cross-link only can happen intrastrand to $G_8$-$G_9$ base in ssDNA **I** (Figure 5a). The formation of such cisplatin cross-linked DNA adduct has been characterized in the previous work using MALDI-TOF-MS analysis.[10] In this situation, a cisPt-DNA-HMGB1a complex with an E-value of -712.2 kcal/mol was simulated. The low interaction energy of the cisplatin damaged DNA and HMGB1a revealed high binding affinity and specificity, which are well consistent with the results from QCM sensing.

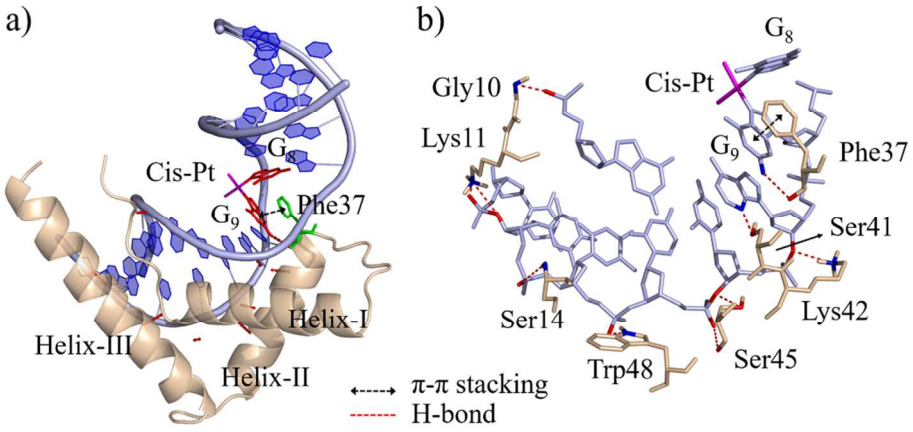


**Figure 5.** The most favorable binding mode of (a) cisPt-DNA-HMGB1a complex (b) π-π stacking interaction and ten hydrogen bonds formed between HMGB1a and cisPt-DNA.

The conformation and non-covalent bonding of the cisPt-DNA-HMGB1a complex were further analyzed based on the docking results together with the QCM data. Basically, the concave surface of HMGB1a binds to the minor groove of DNA duplex. With the 1,2-intrastrand

cross-links by cisplatin, the minor groove in the DNA is widened,[35] and the resultant sharp bend of the duplex becomes more favorable for the accommodation of HMGB1a.[31,46] As indicated in Figure 5b, residues Gly10, Lys11 and Ser14 at N terminal of HMGB1a, Phe37, Ser41, Lys42, Ser45 and Trp48 at Helix II of HMGB1a form multiple hydrogen bonds interaction with the minor groove of DNA duplex. The cooperation effect of such multi-site interactions between amino acids and nucleotides most probably contribute to the fast binding kinetics of HMGB1a with cisPt-DNA ($2.97 \times 10^3$ L $mol^{-1}$ $s^{-1}$). It is also notable the critical roles of Phe37, whose aromatic side chain intercalates into the hydrophobic cleft at the $G_8$-$G_9$ base pair cross-linked by cisplatin. The π-π stacking of the phenyl ring of Phe37 onto $G_9$ base in the cleft further reinforces the interaction and stabilizes the complex, which leads to the difficult dissociation of the complex.

Although molecular docking is a useful tool for analyzing the binding site between biomolecules, it is still a predictive approach for structure analysis. In order to confirm the molecular conformation during interactions, the X-ray crystal structure was further referred.[31,47] With the same DNA sequences and cross-linking methods,[10,15,34] the revealed hydrogen bonding and π-π stacking interaction between cisplatin-damaged DNA and HMGB1a localized at different amino-acid residues and nucleotides are in agreement with those obtained from X-ray crystal result.[31] In complicated biosystems, competitive binding between various protein and DNA is usually kinetically controlled. Those with fast binding kinetics will bind first and play the dominant roles. The attempt to find structural elements affecting the kinetic behavior between cisplatin-damaged DNA and HMGB1a would help understanding the mechanism behind DNA damage response network. The accordance in the structural aspects and kinetic data

from QCM investigation infers the effectiveness and promising perspective of QCM biosensor for the evaluation of the molecular recognition events induced by new DNA damage agents.

## CONCLUSION

A sensitive and highly specific sensor system was tailored for the investigation of dynamic interaction between cisplatin damaged DNA and cellular responsive protein HMGB1 represented by domain A. The integration of flow injection analysis with QCM facilitates the real-time monitoring the time courses of frequency changes induced by the recognition and binding of HMGB1a towards cisplatin damaged DNA in solution. The kinetic parameters, association and dissociation rate constants, demonstrated the rapid formation of cisPt-DNA-HMGB1a complex. The dissociation constant revealed the strong interaction between cisplatin damaged DNA and the cellular responsive protein HMGB1a. Molecular docking results further confirmed the high affinity binding sites between cisplatin damaged DNA and HMGB1a. Such cisPt-DNA-HMGB1a complex can shield the damaged DNA and further block the intracellular DNA repair. The label-free QCM sensor is an ideal tool for studying the specific interaction between drug-damaged DNA and their recognition protein in physiological environment, and will provide a potential sensor platform for rapid screening and evaluating of new DNA-targeting metal anticancer drugs.

## AUTHOR INFORMATION

### Corresponding Author

*Email: zhaorui@iccas.ac.cn. Tel: +86 10 62557910. Fax: +86 10 62559373

*Email: fuyi.wang@iccas.ac.cn

*Email: yyhuang@iccas.ac.cn

## Present Addresses

[#]Yunfeng Xie is currently at China National Cereals, Oils and Foodstuffs Corporation, Beijing, 100020, China

## Author Contributions

The manuscript was written through contributions of all authors. All authors have given approval to the final version of the manuscript.

## Notes

The authors declare no competing financial interest.

## ACKNOWLEDGMENT

Financial supports from National Natural Science Foundation of China (21135006, 21375134, 21475140, 21675161 and 21621062), the Ministry of Science and Technology of China (2015CB856303), and the Chinese Academy of Sciences are gratefully acknowledged.

## REFERENCES

(1) Woo, C. M.; Ranjan, N.; Arya, D. P.; Herzon, S. B. Analysis of Diazofluorene DNA Binding and Damaging Activity: DNA Cleavage by a Synthetic Monomeric Diazofluorene. *Angew. Chem., Int. Ed.* **2014,** *53* (35), 9325-9328.

(2) Lord, C. J.; Ashworth, A. The DNA Damage Response and Cancer Therapy. *Nature* **2012,** *481* (7381), 287-294.

(3) Jung, Y. W.; Lippard, S. J. Direct Cellular Responses to Platinum-Induced DNA Damage. *Chem. Rev.* **2007,** *107* (5), 1387-1407.

(4) Jackson, S. P.; Bartek, J. The DNA-Damage Response in Human Biology and Disease. *Nature* **2009,** *461* (7267), 1071-1078.

(5) Gold, B.; Stone, M. P.; Marky, L. A. Looking for Waldo: A Potential Thermodynamic Signature to DNA Damage. *Acc. Chem. Res.* **2014,** *47* (4), 1446-1454.

(6) Zhang, G. Q.; Huang, H.; Liu, D.; Cheng, Y.; Liu, X. L.; Zhang, W. X.; Yin, R. C.; Zhang, D. P.; Zhang, P.; Liu, J. Z.; Li, C. Y.; Liu, B. D.; Luo, Y. W.; Zhu, Y. X.; Zhang, N.; He, S. M.; He, C.; Wang, H. L.; Chen, D. H. N-6-Methyladenine DNA Modification in Drosophila. *Cell* **2015,** *161* (4), 893-906.

(7) Zhang, C. X.; Chang, P. V.; Lippard, S. J. Identification of Nuclear Proteins That Interact with Platinum-Modified DNA by Photoaffinity Labeling. *J. Am. Chem. Soc.* **2004,** *126* (21), 6536-6537.

(8) Zou, D. D.; Zhang, D. P.; Liu, S. Q.; Zhao, B. L.; Wang, H. L. Interplay of Binding Stoichiometry and Recognition Specificity for the Interaction of MBD2b Protein and Methylated DNA Revealed by Affinity Capillary Electrophoresis Coupled with Laser-Induced Fluorescence Analysis. *Anal. Chem.* **2014,** *86* (3), 1775-1782.

(9) Hughes, E. N.; Engelsberg, B. N.; Billings, P. C. Purification of Nuclear Proteins That Bind to Cisplatin-Damaged DNA - Identity with High Mobility Group Protein-1 and Protein-2. *J. Biol. Chem.* **1992,** *267* (19), 13520-13527.

(10) Du, Z. F.; Luo, Q.; Yang, L. P.; Bing, T.; Li, X. C.; Guo, W.; Wu, K.; Zhao, Y.; Xiong, S. X.; Shangguan, D. H.; Wang, F. Y. Mass Spectrometric Proteomics Reveals that Nuclear Protein

Positive Cofactor PC4 Selectively Binds to Cross-Linked DNA by a trans-Platinum Anticancer Complex. *J. Am. Chem. Soc.* **2014,** *136* (8), 2948-2951.

(11) Reeves, R.; Adair, J. E. Role of High Mobility Group (HMG) Chromatin Proteins in DNA Repair. *DNA Repair* **2005,** *4* (8), 926-938.

(12) Jamieson, E. R.; Lippard, S. J. Stopped-Flow Fluorescence Studies of HMG-Domain Protein Binding to Cisplatin-Modified DNA. *Biochemistry* **2000,** *39* (29), 8426-8438.

(13) Jamieson, E. R.; Jacobson, M. P.; Barnes, C. M.; Chow, C. S.; Lippard, S. J. Structural and Kinetic Studies of a Cisplatin-Modified DNA Icosamer Binding to HMG1 Domain B. *J. Biol. Chem.* **1999,** *274* (18), 12346-12354.

(14) Wannapaiboon, S.; Tu, M.; Fischer, R. A. Liquid Phase Heteroepitaxial Growth of Moisture-Tolerant MOF-5 Isotype Thin Films and Assessment of the Sorption Properties by Quartz Crystal Microbalance. *Adv. Funct. Mater.* **2014,** *24* (18), 2696-2705.

(15) Tsai, W. Y.; Taberna, P. L.; Simon, P. Electrochemical Quartz Crystal Microbalance (EQCM) Study of Ion Dynamics in Nanoporous Carbons. *J. Am. Chem. Soc.* **2014,** *136* (24), 8722-8728.

(16) Jackman, J. A.; Goh, H. Z.; Zhdanov, V. P.; Knoll, W.; Cho, N. J. Deciphering How Pore Formation Causes Strain-Induced Membrane Lysis of Lipid Vesicles. *J. Am. Chem. Soc.* **2016,** *138* (4), 1406-1413.

(17) Timmer, B. J. J.; Flos, M. A.; Jorgensen, L. M.; Proverbio, D.; Altun, S.; Ramstrom, O.; Aastrup, T.; Vincent, S. P. Spatially Well-Defined Carbohydrate Nanoplatforms: Synthesis, Characterization and Lectin Interaction Study. *Chem. Commun.* **2016,** *52* (83), 12326-12329.

(18) Webster, A.; Vollmer, F.; Sato, Y. Probing Biomechanical Properties with a Centrifugal Force Quartz Crystal Microbalance. *Nat. Commun.* **2014,** *5*, 5284.

(19) Cuddy, M. F.; Poda, A. R.; Brantley, L. N. Determination of Isoelectric Points and the Role of pH for Common Quartz Crystal Microbalance Sensors. *ACS Appl. Mater. Interfaces* **2013,** *5* (9), 3514-3518.

(20) Tseng, M. C.; Chu, Y. H. Reaction-Based Azide Gas Sensing with Tailored Ionic Liquids Measured by Quartz Crystal Microbalance. *Anal. Chem.* **2014,** *86* (4), 1949-1952.

(21) Felgueiras, H. P.; Murthy, N. S.; Sommerfeld, S. D.; Bras, M. M.; Migonney, V.; Kohn, J. Competitive Adsorption of Plasma Proteins Using a Quartz Crystal Microbalance. *ACS Appl. Mater. Interfaces* **2016,** *8* (21), 13207-13217.

(22) Cheng, C. I.; Chang, Y. P.; Chu, Y. H. Biomolecular Interactions and Tools for Their Recognition: Focus on the Quartz Crystal Microbalance and Its Diverse Surface Chemistries and Applications. *Chem. Soc. Rev.* **2012,** *41* (5), 1947-1971.

(23) Ma, F.; Rehman, A.; Sims, M.; Zeng, X. Q. Antimicrobial Susceptibility Assays Based on the Quantification of Bacterial Lipopolysaccharides via a Label Free Lectin Biosensor. *Anal. Chem.* **2015,** *87* (8), 4385-4393.

(24) Zhao, Y.; Wang, H. M.; Tang, W.; Hu, S. C.; Li, N.; Liu, F. An in Situ Assembly of a DNA-Streptavidin Dendrimer Nanostructure: A New Amplified Quartz Crystal Microbalance Platform for Nucleic Acid Sensing. *Chem. Commun.* **2015,** *51* (53), 10660-10663.

(25) Zhou, Y. T.; Zhou, P.; Xin, Y. Q.; Wang, J.; Zhu, Z. Q.; Hu, J.; Wei, S. C.; Ma, H. W. Trend of Telomerase Activity Change During Human IPSC Self-Renewal and Differentiation Revealed by a Quartz Crystal Microbalance Based Assay. *Sci. Rep.* **2014,** *4*, 6978.

(26) Deng, X. D.; Chen, M. S.; Fu, Q.; Smeets, N. M. B.; Xu, F.; Zhang, Z. Y.; Filipe, C. D. M.; Hoare, T. A Highly Sensitive Immunosorbent Assay Based on Biotinylated Graphene Oxide and the Quartz Crystal Microbalance. *ACS Appl. Mater. Interfaces* **2016,** *8* (3), 1893-1902.

(27) Zhang, Q. D.; Huang, Y. Y.; Zhao, R.; Liu, G. Q.; Chen, Y. Determining Binding Sites of Drugs on Human Serum Albumin Using FIA-QCM. *Biosens. Bioelectron.* **2008,** *24* (1), 48-54.

(28) Xu, X. H.; Zhou, J.; Liu, X.; Nie, Z.; Qing, M.; Guo, M. L.; Yao, S. Z. Aptameric Peptide for One-Step Detection of Protein Kinase. *Anal. Chem.* **2012,** *84* (11), 4746-4753.

(29) Huang, Y. Y.; Zhang, Q. D.; Liu, G. Q.; Zhao, R. A Continuous-Flow Mass Biosensor for the Real-Time Dynamic Analysis of Protease Inhibition. *Chem. Commun.* **2015,** *51* (30), 6601-6604.

(30) Furusawa, H.; Tsuyuki, Y.; Takahashi, S.; Okahata, Y. In Situ Monitoring of Structural Changes during Formation of 30S Translation Initiation Complex by Energy Dissipation Measurement Using 27-MHz Quartz-Crystal Microbalance. *Anal. Chem.* **2014,** *86* (11), 5406-5415.

(31) Ohndorf, U. M.; Rould, M. A.; He, Q.; Pabo, C. O.; Lippard, S. J. Basis for Recognition of Cisplatin-Modified DNA by High-Mobility-Group Proteins. *Nature* **1999,** *399* (6737), 708-712.

(32) Wang, X.; Xu, J.; Liu, C.; Chen, Y. Specific Interaction of Platinated DNA and Proteins by Surface Plasmon Resonance Imaging. *RSC Adv.* **2016,** *6* (26), 21900-21906.

(33) Xu, D. C.; Min, Y. Z.; Cheng, Q. Q.; Shi, H. D.; Wei, K. J.; Arnesano, F.; Natile, G.; Liu, Y. Z. Chemical and Cellular Investigations of Trans-Ammine-Pyridine-Dichlorido-Platinum(II), the Likely Metabolite of the Antitumor Active Cis-Diammine-Pyridine-Chorido-Platinum(II). *J. Inorg. Biochem.* **2013,** *129*, 15-22.

(34) Liu, Y.; Yu, X.; Zhao, R.; Shangguan, D. H.; Bo, Z. Y.; Liu, G. Q. Quartz Crystal Biosensor for Real-Time Monitoring of Molecular Recognition between Protein and Small Molecular Medicinal Agents. *Biosens. Bioelectron.* **2003,** *19* (1), 9-19.

(35) Takahara, P. M.; Frederick, C. A.; Lippard, S. J. Crystal Structure of the Anticancer Drug Cisplatin Bound to Duplex DNA. *J. Am. Chem. Soc.* **1996,** *118* (49), 12309-12321.

(36) Sauerbrey, G. The Use of Quartz Oscillators for Weighing Thin Layers and for Microweighing. *Z. Phys.* **1959,** *155*, 206-222.

(37) Brewer, S. H.; Glomm, W. R.; Johnson, M. C.; Knag, M. K.; Franzen, S. Probing BSA Binding to Citrate-Coated Gold Nanoparticles and Surfaces. *Langmuir* **2005,** *21* (20), 9303-9307.

(38) Homola, J. Surface Plasmon Resonance Sensors for Detection of Chemical and Biological Species. *Chem. Rev.* **2008,** *108* (2), 462-493.

(39) Xu, D. K.; Xu, D. W.; Yu, X. B.; Liu, Z. H.; He, W.; Ma, Z. Q. Label-Free Electrochemical Detection for Aptamer-Based Array Electrodes. *Anal. Chem.* **2005,** *77* (16), 5107-5113.

(40) Bolduc, O. R.; Masson, J. F. Monolayers of 3-Mercaptopropyl-Amino Acid to Reduce the Nonspecific Adsorption of Serum Proteins on the Surface of Biosensors. *Langmuir* **2008,** *24* (20), 12085-12091.

(41) Farka, Z.; Kovar, D.; Skladal, P. Rapid Detection of Microorganisms Based on Active and Passive Modes of QCM. *Sensors* **2015,** *15* (1), 79-92.

(42) Karpovich, D. S.; Blanchard, G. J. Direct Measurement of the Adsorption-Kinetics of Alkanethiolate Self-Assembled Monolayers on a Microcrystalline Gold Surface. *Langmuir* **1994,** *10* (9), 3315-3322.

(43) Huang, J. C.; Zamble, D. B.; Reardon, J. T.; Lippard, S. J.; Sancar, A. HMG-Domain Proteins Specifically Inhibit the Repair of the Major DNA Adduct of the Anticancer Drug Cisplatin by Human Excision Nuclease. *Proc. Natl. Acad. Sci. U. S. A.* **1994,** *91* (22), 10394-10398.

(44) Pasheva, E. A.; Ugrinova, I.; Spassovska, N. C.; Pashev, I. G. The Binding Affinity of HMG1 Protein to DNA Modified by Cis-Platin and Its Analogs Correlates with Their Antitumor Activity. *Int. J. Biochem. Cell Biol.* **2002,** *34* (1), 87-92.

(45) Macindoe, G.; Mavridis, L.; Venkatraman, V.; Devignes, M. D.; Ritchie, D. W. Hexserver: An FFT-Based Protein Docking Server Powered by Graphics Processors. *Nucleic Acids Res.* **2010,** *38* (Web Server issue), 445-449.

(46) Chow, C. S.; Whitehead, J. P.; Lippard, S. J. HMG Domain Proteins Induce Sharp Bends in Cisplatin-Modified DNA. *Biochemistry* **1994,** *33* (50), 15124-15130.

(47) He, Q.; Ohndorf, U. M.; Lippard, S. J. Intercalating Residues Determine the Mode of HMG1 Domains a and B Binding to Cisplatin-Modified DNA. *Biochemistry* **2000,** *39* (47), 14426-14435.

Table of content